JOURNAL OF FOOD AND DRUG ANALYSIS 26 (2018) 887–902

Available online at www.sciencedirect.com

ScienceDirect

journal homepage: www.jfda-online.com

Original Article

Triple-component nanocomposite films prepared using a casting method: Its potential in drug delivery

Sadia Gilani [a], *Sadullah Mir* [b], *Momina Masood* [a], *Abida Kalsoom Khan* [b], *Rehana Rashid* [b], *Saira Azhar* [a], *Akhtar Rasul* [c], *Muhammad Nadeem Ashraf* [d], *Muhammad Khurram Waqas* [e], *Ghulam Murtaza* [a,*]

[a] *Department of Pharmacy, COMSATS Institute of Information Technology, Abbottabad, Pakistan*
[b] *Department of Chemistry, COMSATS Institute of Information Technology, Abbottabad, Pakistan*
[c] *Department of Pharmaceutics, Faculty of Pharmaceutical Sciences, Government College University, Faisalabad 38000, Pakistan*
[d] *Department of Pharmacology, College of Pharmacy, King Saud University, Riyadh, Saudi Arabia*
[e] *Institute of Pharmaceutical Sciences, University of Veterinary & Animal Sciences (UVAS), Lahore, Pakistan*

ARTICLE INFO

Article history:
Received 26 August 2016
Received in revised form
21 February 2017
Accepted 24 February 2017
Available online 21 March 2017

Keywords:
anti-inflammatory
chitosan
nanocomposite
permeation
polyethylene glycol

ABSTRACT

The purpose of this study was to fabricate a triple-component nanocomposite system consisting of chitosan, polyethylene glycol (PEG), and drug for assessing the application of chitosan–PEG nanocomposites in drug delivery and also to assess the effect of different molecular weights of PEG on nanocomposite characteristics. The casting/solvent evaporation method was used to prepare chitosan–PEG nanocomposite films incorporating piroxicam-β-cyclodextrin. In order to characterize the morphology and structure of nanocomposites, X-ray diffraction technique, scanning electron microscopy, thermogravimetric analysis, and Fourier transmission infrared spectroscopy were used. Drug content uniformity test, swelling studies, water content, erosion studies, dissolution studies, and anti-inflammatory activity were also performed. The permeation studies across rat skin were also performed on nanocomposite films using Franz diffusion cell. The release behavior of films was found to be sensitive to pH and ionic strength of release medium. The maximum swelling ratio and water content was found in HCl buffer pH 1.2 as compared to acetate buffer of pH 4.5 and phosphate buffer pH 7.4. The release rate constants obtained from kinetic modeling and flux values of *ex vivo* permeation studies showed that release of piroxicam-β-cyclodextrin increased with an increase in concentration of PEG. The formulation F10 containing 75% concentration of PEG showed the highest swelling ratio (3.42 ± 0.02) in HCl buffer pH 1.2, water content ($47.89 \pm 1.53\%$) in HCl buffer pH 1.2, maximum cumulative drug permeation through rat skin (2405.15 ± 10.97 μg/cm^2) in phosphate buffer pH 7.4, and *in vitro* drug release ($35.51 \pm 0.26\%$) in sequential pH change mediums, and showed a significantly ($p < 0.0001$) higher anti-inflammatory effect (0.4 cm). It

* *Corresponding author*. Department of Pharmacy, COMSATS Institute of Information Technology, Abbottabad 22060, Khyber PakhtoonKhwa Province, Pakistan.
E-mail address: gmdogar356@gmail.com (G. Murtaza).
http://dx.doi.org/10.1016/j.jfda.2017.02.006

can be concluded from the results that film composition had a particular impact on drug release properties. The different molecular weights of PEG have a strong influence on swelling, drug release, and permeation rate. The developed films can act as successful drug delivery approach for localized drug delivery through the skin.

1. Introduction

Modified drug delivery system (MDDS) means release of drug from a drug delivery system that is modified in some way [1]. MDDS includes transdermal drug delivery system, controlled or sustained released dosage form and delayed released dosage form. MDDSs are preferable to conventional drug delivery systems because of certain advantages such as improved patient compliance and comforts owing to reduced dosing frequencies, more efficient drug therapy to patients, and more uniform drug therapeutic levels [2].

Nanocomposites are composed of either multiple nanoscale substances or a single entity of nanoscale material that is incorporated into the bulk material. These nanocomposites may come in different combinations, i.e., two hard nanomaterials, two soft nanomaterials, or a combination of hard and soft nanomaterial [3]. Based on the nature of the matrix, the nanocomposites have been categorized as metal, ceramic, and polymer matrix nanocomposites [4]. Among all, polymer matrix-based nanocomposites have been formulated by different techniques including sol–gel reaction, solvent casting, extrusion, and dispersion of clays into the polymer matrices [5]. Solvent casting is mainly a manufacturing process where a filler and a solubilized polymer matrix are mixed together by creating agitation through the use of mechanical stirrer. This mixing is followed by casting and solvent removal via evaporation or any other drying methods [6].

Biodegradable polymers are used as biomaterials in numerous techniques, particularly in tissue engineering, gene therapy, wound healing, and controlled drug delivery systems. These biodegradable polymers are important in such a way that the implanted foreign materials vanish from the body as a result of their degradation. Examples of the most commonly used biodegradable polymers in biomedical applications are polylactic acid, polyethylene glycol (PEG), polyglycolic acid, poly-ε-caprolactone, poly-3-hydroxybutyrate, copolymers of polyglycolide, chitosan, alginate, and soy protein [7]. PEG is a biodegradable polymer with excellent properties such as biocompatibility and safety. It is used in combination with other polymers to formulate controlled release drugs [8]. The second most abundant polysaccharide in nature is chitosan, the cationic (1–4)-2-amino-2-deoxy-β-D-glucan. Chitosan of different quality grades can be produced from chitin. Chitosan has great importance because of its biodegradability, biocompatibility, and nontoxicity [9].

Organic polymer matrixes and nanoscale-organophilic clay fillers make up a group of amalgam materials, i.e., polymer–clay nanocomposites [10]. In order to improve the blend properties, it has been suggested that nanoclays can improve the compatibility of immiscible polymers [11]. Sepiolite $[Si_{12}O_{30}Mg_8(OH)_4(OH_2)_4 \cdot 8H_2O]$ is a fibrous hydrated magnesium silicate. Its structure is related to montmorillonite comprising octahedral layers of magnesium oxide/hydroxide inserted between two tetrahedral silica layers. The only difference between montmorillonite and sepiolite is the lack of continuous octahedral sheets [12]. Previously, it was used as filler for the formulation of polymer–clay nanocomposites [13].

Transportation of drug molecules through the skin undergoes two processes: drug penetration through the stratum corneum followed by drug diffusion into deeper tissues. The rate and extent of drug transportation depends on hydrogen bonding, size, ionic strength, log *P* (the partition coefficient of a molecule between an aqueous and lipophilic phases, usually octanol and water), and physicochemical properties [14].

Piroxicam-β-cyclodextrin belongs to the class of nonsteroidal anti-inflammatory drugs (NSAIDs). This drug has many pharmacological roles, but the most important are its analgesic and antipyretic functions. At present, this drug is available in tablet and capsule dosage forms and is thus administered orally. However, prolonged oral administration of these dosage forms may result in many life-threatening effects including epigastric pain, heartburn, gastrointestinal bleeding, aplastic anemia, renal damage, hematuria, purpura, pemphigus vulgaris, and anaphylactic shock [15]. The rare adverse effects of piroxicam-β-cyclodextrin include bladder dysfunction, erythema multiforme (Stevens–Johnson syndrome), alopecia, toxic epidermal necrolysis or Lyell's syndrome, stomatitis, agranulocytosis, and nail growth problems [16]. These side effects can be eliminated by delivering this transdermally drug through skin.

In order to overcome these side effects, we report a new formulation of piroxicam-β-cyclodextrin as nanocomposite films. These nanocomposite films can produce controlled release therapeutic effect with negligible side effects. Such type of formulations with minimal side effects may play an important role for the pharmaceutical industry. The purpose of this study was to assess the applications of chitosan–PEG nanocomposites in drug delivery and also to assess the applications of different molecular weights of PEG in drug delivery in the form of nanocomposites with chitosan.

2. Methods

2.1. Materials

Chitosan was purchased from Sigma-Aldrich (St. Louis, Missouri, USA). Its density ranges from 0.15 g/cm^3 to 0.3 g/cm^3.

PEG in three different molecular weights (750, 2000, and 5000) was purchased from Sigma-Aldrich. Sepiolite was supplied by International Laboratory (St. Louis, Missouri, USA). Glacial acetic acid (≥99.85%) having a freezing point of 16.35°C was colorless and clear, and glycerol with a molecular weight of 92.09, density of 1.26 g/mL, and melting point of 17.8°C that was used as plasticizer was purchased from Sigma-Aldrich. Potassium chloride and sodium hydroxide with a purity of 99% was purchased from Sigma-Aldrich. Sodium acetate was purchased from Merck (Darmstadt, Germany). Potassium dihydrogen phosphate (KH_2PO_4) was purchased from Daejung Chemical & Metal Co. (Shiheung, South Korea). Piroxicam-β-cyclodextrin was a gift from Weatherfolds Pharmaceutical (Hattar, Pakistan). Fresh deionized distilled water was prepared in the COMSATS laboratory, Abbottabad, Pakistan.

2.2. Preparation of chitosan–PEG nanocomposites

Drug-loaded polymeric nanocomposites were prepared by making a slight modification in the previously reported solvent casting technique [8]. First, PEG was allowed to dissolve completely in 1% aqueous acetic acid solution followed by the gradual addition of chitosan and glycerol (as plasticizer) with constant stirring until a homogeneous solution was obtained. Then, reinforcement agent, i.e., nanoclay, was added to the polymer mixture and, after 15 minutes, piroxicam-β-cyclodextrin was poured to the same solution while stirring constantly. The solution was allowed to stir for about 30 minutes at 60°C until a clear solution was achieved. After complete dissolution, the resulting mixture was poured into Petri dishes of uniform diameter and placed in an oven at 40°C for 24 hours for complete drying. After drying, a hard smooth plastic type film was obtained. Twenty-two different formulations were prepared by varying the quantity of polymer and glycerol in accordance with the study design as noted in Table 1.

2.3. Characterization of formulations

The formulated nanocomposite films containing piroxicam-β-cyclodextrin were subjected to the following tests for evaluation of film properties.

2.3.1. Fourier transform infrared spectroscopy

To observe the possibility of intermolecular bonding between adjunct piroxicam-β-cyclodextrin molecules, Fourier transform infrared (FTIR) was used. Thermo Scientific Nicolet 6700" Fourier Transform Infrared Spectrophotometer (Thermo Electron Corporation, MA, USA) was used for the structural examination of nanocomposite films. All samples were grounded and mixed thoroughly with potassium bromide. The spectrum was scanned from 4000 cm^{-1} to 500 cm^{-1} [17].

2.3.2. Thermal analysis

Thermal and compositional analysis was performed to evaluate the decomposing kinetics of piroxicam-β-cyclodextrin nanocomposites. The thermal stability of nanocomposite films was estimated using Thermal Analyzer (Shimadzu DTG-60H, Nottinghamshire, NG12 5AW, United Kingdom). Under a nitrogen atmosphere with a constant flow rate of about 20 mL/min, nanocomposite films were subjected to analytical pan. Approximately 4 mg of the sample was positioned in an aluminum pan, then thermal decomposition of sample was carried out at 0–700°C. The continuous weight loss and temperature was noted and analyzed [18].

Table 1 – Formulation development design.

Formulation codes	Chitosan/PEG (100 parts)	Sepiolite (PHR)	Piroxicam-β-cyclodextrin (PHR)	Glycerol (PHR)
Chitosan/PEG 750				
F1	100:0	3	10	50
F2	75:25	3	10	50
F3	50:50	3	10	50
F4	25:75	3	10	50
F5	0:100	3	10	50
F6	50:50	3	0	50
Chitosan/PEG 2000				
F7	100:0	3	10	50
F8	75:25	3	10	50
F9	50:50	3	10	50
F10	25:75	3	10	50
F11	0:100	3	10	50
F12	50:50	3	0	50
F13	75:25	3	10	70
F14	75:25	3	10	30
F15	75:25	3	10	10
F16	75:25	3	10	0
Chitosan/PEG 5000				
F17	100:0	3	10	50
F18	75:25	3	10	50
F19	50:50	3	10	50
F20	25:75	3	10	50
F21	0:100	3	10	50
F22	50:50	3	0	50

PEG = polyethylene glycol; PHR = parts per hundred.

2.3.3. X-ray diffraction

The crystallinity of the piroxicam-β-cyclodextrin nanocomposites was determined using X-ray diffraction (XRD) test. To identify the physical form (crystalline or amorphous) of nanocomposite films, X-ray diffractometer Philips XPERT PRO 3040/60 was used. The scanning range of 2θ was 5–90°.

2.3.4. Scanning electron microscopy

A scanning electron microscope (JSM 6400F; Jeol, Tokyo, Japan) was used to study the surface morphology of nanocomposite films, operated at a voltage range of 5–15 kV. With the help of a sticky carbon tape, the samples were placed on an aluminum holder and by gold stammer; a thin layer of gold was coated on it [19].

2.3.5. Energy dispersive X-ray analysis

Energy dispersive X-ray (EDX) analysis was also performed through the scanning electron microscope (JSM 6400F SEM; Jeol). The film samples were deposited on an aluminum holder with the help of a sticky carbon tape, and a thin layer of gold was coated on it using a gold stammer. We used a voltage of 20.194 kV for EDX analysis. The EDX spectrum was measured in a spot profile mode by concentrating the electron ray onto particular regions of the sheet. EDX analysis was done to observe the elemental composition of matrix and purity of mixing components.

2.4. Preliminary solubility studies of piroxicam-β-cyclodextrin

Solubility studies were performed using different solvents. Piroxicam-β-cyclodextrin was added in sufficient amount to 50 mL of various solvents. Then, these solutions were stirred for 24 hours at 37 ± 0.5°C. After stirring, the samples were centrifuged (heraeus megafugr 8R; Thermofisher Scientific Lab Centrifuge, Zweigniederiassung Osterode, Osterode am Harz, Germany) for 10 minutes at 4193 × *g* to eliminate the extra quantity of piroxicam-β-cyclodextrin. The supernatant layer was filtered and properly diluted with respective solvents. The concentration of piroxicam-β-cyclodextrin was determined spectrophotometrically (O.R.1 3000, UV–visible spectrophotometer, Iba, Göttingen, Germany) at 207 nm using specific solvent as a blank [20].

2.5. Construction of calibration curve

To obtain a linear equation, the standard calibration curve of piroxicam-β-cyclodextrin was constructed that was used to estimate the concentration of piroxicam-β-cyclodextrin in further studies. For this purpose, a stock solution of piroxicam-β-cyclodextrin was obtained by mixing 100 mg of piroxicam-β-cyclodextrin in 100 mL phosphate buffer pH 7.4, and serial dilutions were prepared (ranging from 1 μg/mL to 9 μg/mL) in the same buffer. The solutions were analyzed spectrophotometrically at 207 nm using the same buffer as a blank [21].

2.6. Drug content uniformity

A specific quantity (40 mg) of nanocomposites film was placed in a 100-mL volumetric flask, and the volume was adjusted up to the mark with phosphate buffer pH 7.4 and stirred (LMS-1003; Daihan Labtech Co., Gyeonggi-do, Korea) for 24 hours. After 24 hours, the dilutions were made from the solution, and absorbance was estimated spectrophotometrically at 207 nm using phosphate buffer pH 7.4 as blank [21].

2.7. Swelling studies

The swelling studies of nanocomposite films were performed in three different buffers (with pH 1.2, 4.5, and 7.4). The accurately weighed 50 mg of nanocomposite films was placed in Petri dishes containing 30 mL buffers with pH 1.2, 4.5, and 7.4. After 15 minutes, 30 minutes, 60 minutes, 90 minutes, and 120 minutes, the films were removed from Petri dishes and lightly stained with tissue in order to remove the extra buffer and weighed (PA214; Ohaus Corporation, Parsippany, NJ, USA). The degree of swelling at each time point was weighed for each sample. The experiment was carried out in triplicate. The water content (%) and swelling ratio (SR) was determined using the following equations [22]:

$$SR = W_s/W_d \quad (1)$$

$$\text{Water content } (\%)[W_s - W_d/W_s] \times 100, \quad (2)$$

where W_d is the weight of dry films and W_s is the weight of swollen films.

2.8. Erosion studies

After performing swelling studies, erosion studies were performed. Each swollen sample was dried in an oven at 40°C for 12 hours, and each sample was individually weighed (PA214; Ohaus Corporation) at different time intervals until constant mass was attained. The test was carried out in triplicate. The film erosion (%) at different time intervals was calculated as follows [23]:

$$\text{Film erosion } (\%) = (W_0 - W_2/W_0) \times 100, \quad (3)$$

where W_0 is the weight of wet swollen films and W_2 is the final dry weight.

2.9. Preparation of rat skin

Fifty Sprague–Dawley rats were obtained from the animal house of COMSATS Institute of Information and Technology, Abbottabad, Pakistan; their approximate average weight was 200–250 g. The animals stay retained on a 12-hour light/12 dark cycle and nitrified with standard food and water *ad libitum* [24]. The study was performed after institutional approval was obtained (Department of Pharmacy, COMSATS institute of Information and Technology). The use of animals in the experimental study design was in accordance with Good Clinical practice [24].

Rats were anesthetized using chloroform. The belly skin was carefully shaven with an electrical and hand blade; then the skin was surgically detached, and supporter dermal fats were cleaned. The skin was kept in 0.9% NaCl solution (normal saline solution) for 2 hours to remove leachable enzymes and extraneous debris. After washing with disinfected water, the

cleaned skin was enfolded in aluminum sheet and stored at −20°C until use. On the day of the experiment, the frozen excised skin was brought to room temperature and was fixed among donor and the receptor compartments of the Franz diffusion cell with the stratum corneum side facing toward the donor compartment and the dermal side toward the receptor compartment [14].

2.9.1. Ex vivo *permeation studies*

Drug permeation from the film was performed on rat skin using Franz diffusion cell [25]. The receptor compartment was filled with phosphate buffer pH 7.4. The rat skin was mounted among the donor and receptor compartments of the Franz cell. The two cell compartments were held together with clamps. Then, 40 mg of the nanocomposite film containing 2.5 mg drug was placed in the donor compartment and was enclosed with aluminum foil to prevent drying. The receptor solution was continuously stirred (LMS-1003; Daihan Labtech Co.) by means of a stirring bar magnet. The temperature of the Franz cell was maintained at 37 ± 0.5°C. The liquid samples were obtained from the receptor compartment at fixed time intervals of 0.25 hour, 0.5 hour, 1 hour, 2 hours, 4 hours, 8 hours, 12 hours, and 24 hours, and were substituted with equal volumes of fresh phosphate buffer (pH 7.4) to retain the sink condition. The amount of piroxicam-β-cyclodextrin in the samples was analyzed spectrophotometrically (O.R.I 3000, UV–visible spectrophotometer) at 207 nm using the same buffer as a blank.

2.9.2. *Permeability data analysis*

Permeability studies of the prepared formulations were also conducted for the purpose of observing the transdermal penetration of drug from formulations through the skin. Permeability coefficient and steady-state flux were calculated from *ex vivo* permeation data.

2.9.2.1. *Steady-state flux*. The steady-state flux was calculated using the following equation:

$$\text{Steady} - \text{state flux } (J_{SS}) = dM/S.dt, \tag{4}$$

where dM is equal to the quantity of drug that permeated across a unit cross section area (S), per unit time (t) [14].

2.9.2.2. *Permeability coefficient*. The permeability coefficient (K_p) across the membrane was calculated using the following equation:

$$\text{Permeability coefficient } (K_p) = J_{SS}H/C_0, \tag{5}$$

where H is the width of the membrane and C_0 is the original drug concentration [14].

2.10. *Dissolution studies*

The dissolution studies were performed using USP Apparatus II (USP rotating paddle method). First, 100 mg nanocomposite films were suspended in 900 mL dissolution media of pH 1.2, 6.8, and 7.4 buffer solutions. The dissolution medium was constantly stirred at 50 rpm. The experiment was performed by using the HCl buffer pH 1.2 medium for 2 hours and then substituted with new phosphate buffer of pH 6.8 medium for the next 3 hours. After 3 hours, the dissolution medium was again replaced with fresh phosphate buffer pH 7.4, and the dissolution process was continued for a further 7 hours. The whole study was performed at 37 ± 0.5°C for 12 hours. At predetermined time intervals, 5-mL samples were withdrawn for analysis, and the same volume was replaced with fresh dissolution medium. Withdrawn samples were analyzed spectrophotometrically (O.R.I 3000, UV–visible spectrophotometer) at 207 nm [26].

2.10.1. In vitro *drug release kinetics*

The *in vitro* drug release kinetics of piroxicam-β-cyclodextrin from the prepared nanocomposite films was determined by applying various model-dependent and -independent approaches [27].

In model-dependent approaches, the following models were applied to estimate the drug release pattern from nanocomposite films.

$$\text{Zero} - \text{order model} : Q_t = Q_0 = K_0 \times t, \tag{6}$$

where Q_t is the percentage drug release at time t, K_0 is the zero-order release rate constant (unit is concentration/time), t is time, and Q_0 is the quantity of drug remaining undissolved at time t.

$$\text{First} - \text{order model} : \ln Q_0 = \ln Q_t - K_f \times t, \tag{7}$$

where Q_t is the percentage drug release at time t, Q_0 is the original drug concentration, K_f is the first-order release rate constant (unit is time^{-1}), and t is time.

$$\text{Higuchi release model} : Q_t = K_h t^{1/2}, \tag{8}$$

where Q_t is the percentage drug release at time t, K_h is the Higuchi release rate constant, and t is time.

$$\text{Korsmeyer} - \text{Peppas model} : Q_t/Q_0 = K_{kp} t^n, \tag{9}$$

where Q_t/Q_0 is the drug fraction released at time t, K_{kp} is the Korsmeyer–Peppas release rate constant, t is time, and n is the release exponent that indicates the mechanism of drug release.

The release exponent (n) from its regression equation was used to describe the drug release mechanism as described in Table 2.

In model-independent approaches, evaluation of similarity factor (f_2) was conducted. Similarity factor (f_2) was used to check the dissolution profile equivalency of prepared formulations. This method was applied to compare the *in vitro* dissolution profiles of formulations with different grades of PEG. The similarity factor (f_2) was calculated by using the following equation:

Table 2 – Release exponents and drug release mechanism.

Release exponent (n)	Drug release mechanism
0.45	Fickian diffusion
$0.45 < n > 0.89$	Non-Fickian diffusion (anomalous)
0.89	Case II transport
>0.89	Super Case II Transport

$$f_2 = 50\log\left\{\left[1 + 1/nW_t\sum_{t=1}^{n}(R_t - T_t)^2\right]^{-0.5} \times 100\right\}, \quad (10)$$

where n is the number of data points, W_t is the optional weight factor, R_t is the percent drug dissolved in reference at time t, and T_t is the percent drug dissolved in test at the same time t. For alike dissolution profiles, the similarity factors should be in the range of 50–100.

2.11. Anti-inflammatory activity

Formulations F4, F10, and F20 were selected on the basis of their higher flux to evaluate anti-inflammatory activity. The anti-inflammatory activity of the selected films were determined and compared with the control formulation without model drug. In this experiment, male Sprague–Dawley rats (weighing 180–200 g) were used. The activity was conducted using carrageenan-induced hind paw edema method. Rats were selected randomly and distributed into four groups, with each group having four rats. On the day prior to application of formulations, the hairs on dorsal surface of the rats were removed. On the day of application of the formulations, F4, F10, F20, and control formulation were applied by mild rubbing for 15 seconds on shaved dorsal surfaces of rats. After 5 hours, 0.1 mL of 1% w/v carrageenan solution previously prepared in normal saline was administered into the subplantar region of the right hind paw of all treated and control rat groups. The volume of edema was measured in terms of paw thickness in all four rat groups after 2 hours, 4 hours, and 6 hours of administration of carrageenan injection with the help of Vernier caliper [14].

2.12. Data analysis

One-way analysis of variance was used to analyze the anti-inflammatory activity.

3. Results

3.1. FTIR spectroscopy

FTIR spectra of nondrug- and drug-loaded nanocomposite films had been studied in order to investigate the variation in the frequency shift of the functional group. The frequency shift showed the interaction of mixing components. Figure 1 shows the FTIR spectra of drug-loaded and nondrug-loaded chitosan–PEG based nanocomposites.

The characteristic peak of OH-stretching frequency was observed in all samples as shown in Table 3. It appeared at 3353 cm^{-1}, 3305 cm^{-1}, and 3268 cm^{-1} for F6, F12, and F22, respectively. The drug containing samples F3, F9, and F19 showed OH-stretching frequency at 3282 cm^{-1}, 3265 cm^{-1}, and 3260 cm^{-1}, respectively. The nondrug-loaded formulations (F6, F12, and F22) showed higher frequency shift for the OH peak, whereas the drug-loaded samples (F3, F9, and F19) showed lower frequency shift for the OH peak. The OH peak of drug-loaded formulations was broader as compared to the OH band of sample that is nondrug-loaded, which was attributed to the

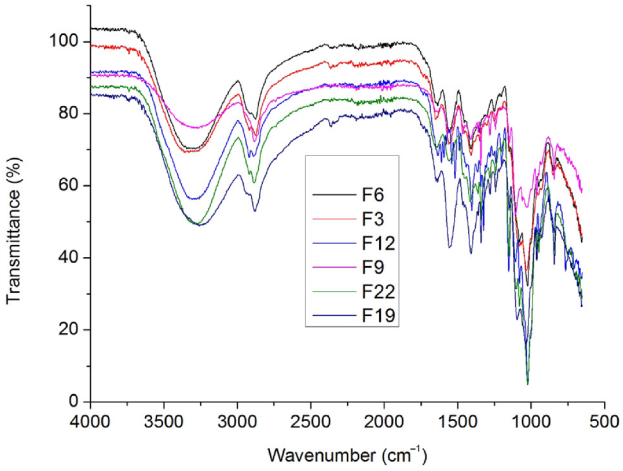

Figure 1 – FTIR spectra of F6, F3, F12, F9, F22, and F19 chitosan–PEG nanocomposite films. FTIR = Fourier transform infrared; PEG = polyethylene glycol.

strong hydrogen bonding and intermolecular interactions of samples with drug. This showed that addition of drug increases the intermolecular interactions. The amide II peak is relatively stable in all samples except F9, which showed the maximum lower frequency shift at 1540 cm^{-1}. This means that the polymers were highly compatible in F9. Antisymmetric stretching peaks of drug had been observed in F3, F9, and F19 at 1251 cm^{-1}, 1239 cm^{-1}, and 1241 cm^{-1}, respectively. The lower frequency shift was observed for F9; this interaction clearly indicated the compatibility of drug with matrix. Similarly, the siloxane (Si–O–Si) peak of F9 formulation was observed at a lower frequency of 1020 cm^{-1}. This lower frequency shift also confirmed the strong interaction of sepiolite with mixing components.

3.2. Thermal analysis

Figure 2 shows the thermogravimetric analysis (TGA) reports of drug-loaded and nondrug-loaded formulations. Table 4 shows the three stages of degradation ranging from 0°C to 150°C, 150°C to 200°C, and 250°C to 400°C. The residues were observed at 600°C. At 150°C, the nondrug-loaded formulations showed the least thermal stability, and F22 showed the maximum thermal stability of 21.58% whereas F6 showed the minimum thermal stability of 22.88%. The drug-loaded formulations showed the higher thermal stability, and F19 showed the maximum thermal stability of 17.38% whereas F3 showed the minimum thermal stability of 22.19%. The drug-loaded formulations showed the higher thermal [stability as compared to nondrug-loaded formulations at 150°C. At 200°C, the nondrug-loaded formulations showed the least thermal stability, and formulation F22 showed the maximum thermal stability of 36.28% whereas F12 showed the minimum thermal stability of 38.89%. The drug-loaded formulations showed the higher thermal stability, and formulation F9 showed the maximum thermal stability of 31.32% whereas F3 showed the minimum thermal stability of 35.28%. The drug-loaded formulations showed the higher thermal stability as compared to nondrug-loaded formulations at 200°C. At 400°C,

Table 3 – FTIR peaks of some important functional groups.

S. No.	Functional group				Observed values (cm^{-1})					
	Chitosan	PEG	Drug	Clay	F6	F3	F12	F9	F22	F19
1	–OH stretching (3430 cm^{-1})	–OH stretching (3421 cm^{-1})	–OH stretching (3391 cm^{-1})	–OH stretching (3688 cm^{-1})	335	3282	3305	3265	3268	3260
3	Amide I (C=O) (1650 cm^{-1})	…	…	…	1647	1635	1633	1634	1635	1648
4	Amide II (N–H bending) (1580 cm^{-1})	…	…	…	1559	1558	1551	1540	1558	1558
5	…	…	O=S=O (1210–1260 cm^{-1})	…	—	1251	—	1239	—	1241
6	…	…	…	Si–O–Si (1000–1068 cm^{-1})	1036	1030	1026	1020	1035	1040

FTIR = Fourier transform infrared; S. No. = sample number.

the nondrug-loaded formulations showed the least thermal stability, and F12 showed the maximum thermal stability of 70.21% whereas F6 showed the minimum thermal stability of 98.09%. The drug-loaded formulations showed the higher thermal stability, and F9 showed the maximum thermal stability of 62.22% whereas F19 showed the minimum thermal stability of 66.22%. The drug-loaded formulations showed the higher thermal stability as compared to nondrug-loaded formulations at 400°C. The weight residues were observed at 600°C. The minimum residues were observed for F6, which were 2%, and maximum residues were observed for F9, which were 37.78%. The remaining residues showed that drug-loaded formulations were thermally stable as compared to nondrug-loaded formulations.

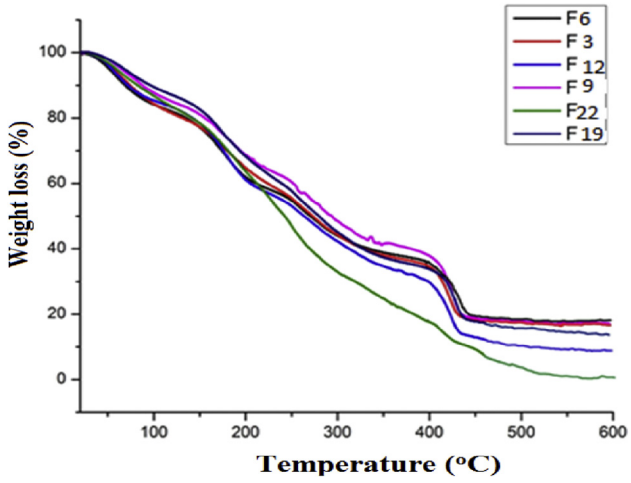

Figure 2 – TGA thermograms of F3, F6, F9, F12, F19, and F22 of chitosan–PEG nanocomposite films. PEG = polyethylene glycol; TGA =thermogravimetric analysis .

Table 4 – Percentage mass loss of F3, F6, F9, F12, F19, and F22 at different temperature ranges.

Formulation codes	Mass loss (%) at 150°C	Mass loss (%) at 200°C	Mass loss (%) at 400°C	Residue (%) at 600°C
F6	22.88	38.12	98.09	2.0
F3	22.19	35.28	65.38	34.65
F12	21.59	38.89	70.21	29.79
F9	18.99	31.32	62.22	37.78
F22	21.58	36.28	82.30	17.70
F19	17.38	31.71	66.22	33.78

3.3. *X-ray diffraction*

Figure 3 shows the XRD diffractograms of nondrug-loaded and drug-loaded formulations. XRD studies were carried out to observe the physical nature of prepared nanocomposites—whether they were crystalline or amorphous.

Previous studies showed that both PEG and chitosan were crystalline. The XRD pattern of nondrug-loaded samples F6, F12, and F22 showed a characteristic sharp peaks at ($2\theta = 20.60°$), ($2\theta = 23.22°$), ($2\theta = 18.83°$, $23.00°$). It showed that characteristic peaks of chitosan as well as PEG were present and explained the strong interaction between chitosan and PEG.

In the drug-loaded samples, the 2θ value was decreasing and d spacing values were increasing in all samples as compared to nondrug-loaded samples (Table 5). This indicates that addition of drug had decreased the crystallinity of samples. Because piroxicam-β-cyclodextrin was amorphous in

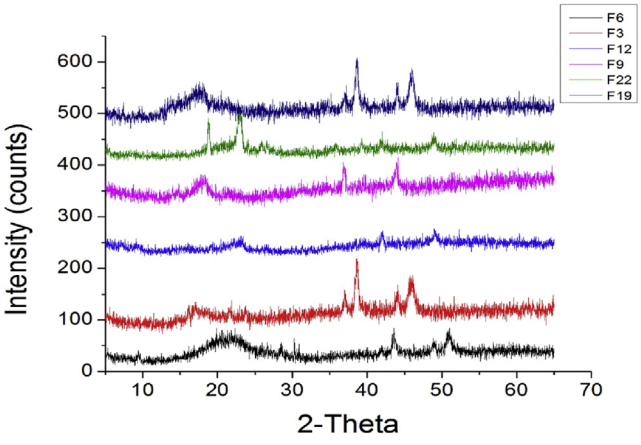

Figure 3 – XRD patterns of F6, F3, F12, F9, F22, and F19 chitosan–PEG nanocomposite films. PEG = polyethylene glycol; XRD = X-ray diffraction.

Table 5 – Comparison of *d* spacing and intensity of curves against 2θ when polymer grade varies.

S. No	Formulation codes	2θ	Intensity	*d* spacing
1	F6	20.60	78.14	4.3
2		43.50	79.91	2.0
3		50.87	83.11	1.7
1	F3	16.75	132.1	5.4
2		38.59	214.0	2.3
3		46.08	182.0	1.9
1	F12	23.22	257.86	3.8
2		42.09	267.45	2.1
3		49.05	276.69	1.8
1	F9	18.05	380.0	4.6
2		36.92	400.65	2.4
3		44.28	413.0	2.0
1	F22	18.83	481.99	4.7
2		23.08	494.42	3.8
3		41.83	454.64	21
4		48.94	459.61	1.8
1	F19	17.53	559.0	4.9
2		38.71	604.18	2.3
3		45.82	585.0	1.9

S. No. = sample number.

nature, its addition in chitosan–PEG matrix increased the amorphous growth of PEG and chitosan.

3.4. *Scanning electron microscopy*

The scanning electron micrographs of F12 and F6 at two different magnification settings are shown in Figures 4 and 5.

Figures 4 and 5 show that the filler was uniformly distributed throughout the polymer matrix. No gap was observed, showing that the filler was fully compatible with the polymer matrix. At high resolution, small spots were observed that responded to clay nanoparticles, which were fully compatible with polymer matrix. The particle small size ranging from 300 nm to 500 nm was attributed to sepiolite particles. However, some large particles were also seen in the matrix. These large particles were integrated clay bundles that were not fully dispersed in the matrix.

3.5. *EDX analysis*

The elemental composition of formulation F9 was studied with EDX (Table 6). Figure 6 shows the EDX analysis.

It was observed that elements revealed the purity of mixing components. The peak of sulfur corresponded to a drug that was of low intensity as the drug was used in small quantity. The peaks of Ca, Mg, and Si corresponded to sepiolite. The peaks of C, N, and O corresponded to polymers, which were of high intensity as polymers were used in high concentrations.

3.6. *Preliminary solubility studies of piroxicam-β-cyclodextrin*

The saturation solubility of a weakly acidic drug, piroxicam-β-cyclodextrin, was determined at room temperature (i.e., at 25°C) in various solvents as listed in Table 7. As shown in Table 7, the highest solubility of piroxicam-β-cyclodextrin was found in phosphate buffer solution pH 7.4. Therefore, phosphate buffer pH 7.4 was selected for further studies.

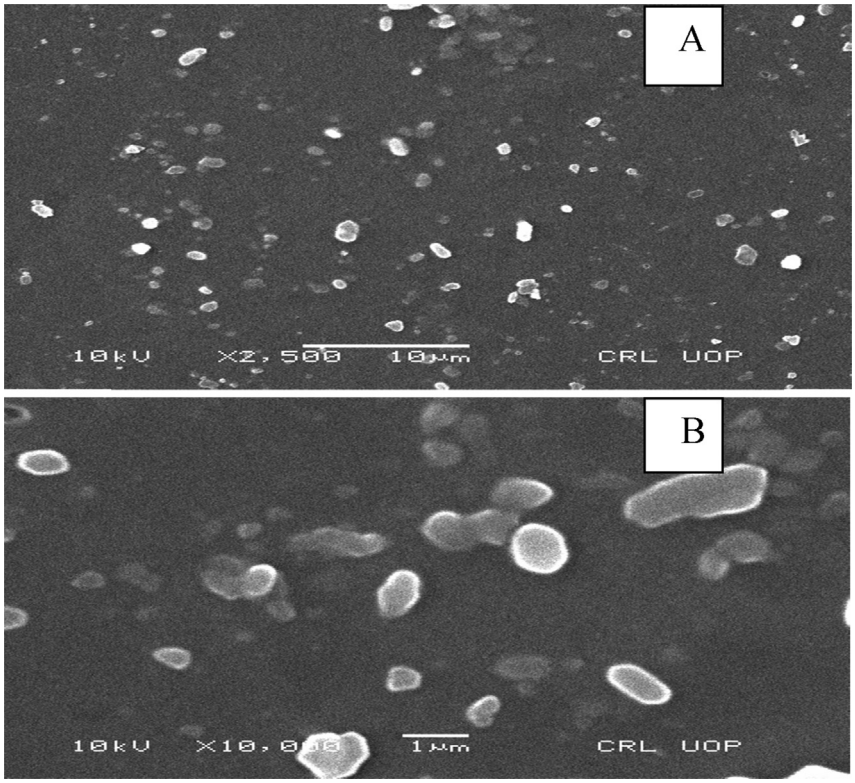

Figure 4 – Scanning electron micrograph of formulation F12. (A) Magnification, ×500. (B) Magnification, ×10,000.

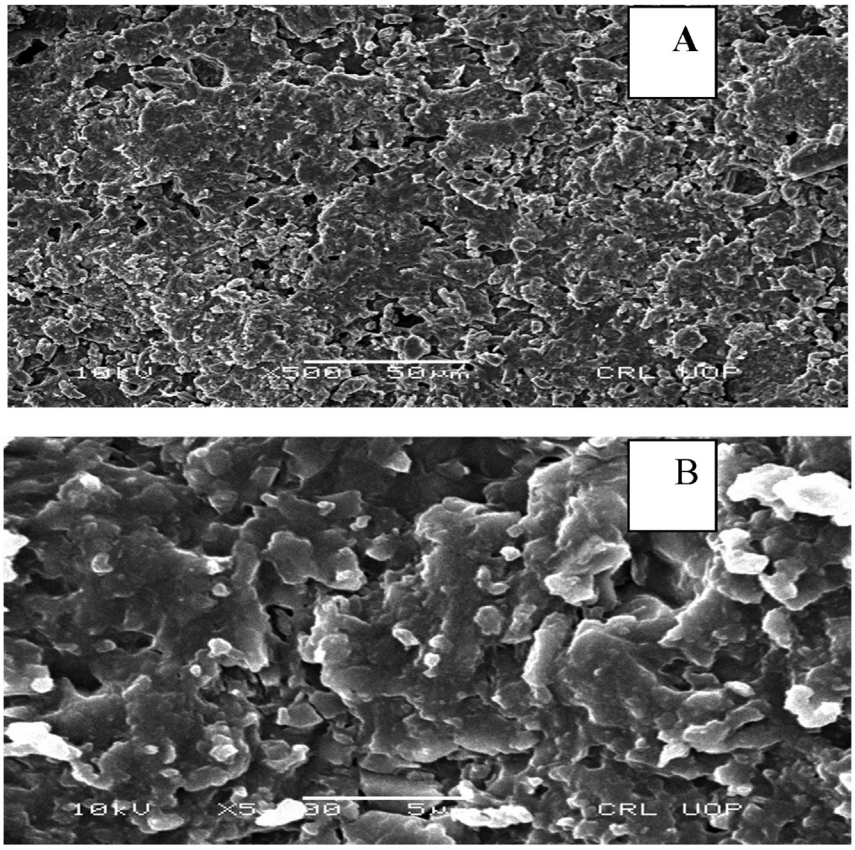

Figure 5 – Scanning electron micrograph of formulation F9. (A) Magnification, ×500. (B) Magnification, ×5000.

3.7. *Preparation of standard curve*

A calibration curve of piroxicam-β-cyclodextrin was constructed by making a series of dilutions ranging from 1 μg/mL to 9 μg/mL in phosphate buffer pH 7.4. The obtained y equation was $0.0731x + 0.0236$, with a coefficient of determination (R^2) of 0.9984 (Figure 7).

3.8. *Drug loading efficiency and drug content uniformity test*

The drug content uniformity for selected formulations was carried out using phosphate buffer pH 7.4. Details of the drug contents of drug-loaded formulations are presented in Table 8.

Table 8 shows that formulation F10 (~99%) showed the maximum drug loading efficiency, whereas F1 (~93%) showed the minimum drug loading efficiency. The nonsignificant difference was observed between contents in the center and contents in proximity, which showed that the drug was uniformly distributed throughout the nanocomposite films.

Table 6 – Elemental composition of formulation F9.

Element	Weight (%)
Carbon	39.95
Nitrogen	10.99
Oxygen	45.17
Magnesium	1.00
Silica	1.75
Sulfur	0.41
Calcium	0.73
Total	100.0

3.9. *Swelling studies and water content*

The swelling behavior and water content of nanocomposite films were studied in different buffers (at pH 1.2, 4.5, and 7.4), and results obtained are given in Figures 8 and 9.

The swelling and water content behavior of nanocomposite films were evaluated in different buffers having pH of 1.2, 4.5, and 7.4. It was observed that the swelling ratio and water content of all films were higher in pH 1.2 as compared to pH 4.5 and 7.4 regardless of the PEG grade used. It was found that swelling ratio and percentage water content were increased by decreasing the amount of chitosan, as the highest solubility ratio and water content was found in formulation F10 (3.42 ± 0.02, $47.89 \pm 1.53\%$) in HCl buffer pH 1.2, which contains 75% concentration of PEG, and formulation F1 (1.78 ± 0.14, $43.64 \pm 4.47\%$) showed the smallest swelling ratio and percentage water content containing 0% PEG. Similar results were observed with other grades of PEG 750 and PEG 5000 used in variable concentrations with respect to chitosan. The higher swelling ratio was observed in PEG 2000, then in PEG 750, and then in PEG 5000. So, the formulations containing PEG 2000 showed the maximum swelling ratio and water content as compared to PEG 750 and PEG 5000. Formulation F16 was decomposed during swelling studies in buffers having pH 1.2 and 4.5.

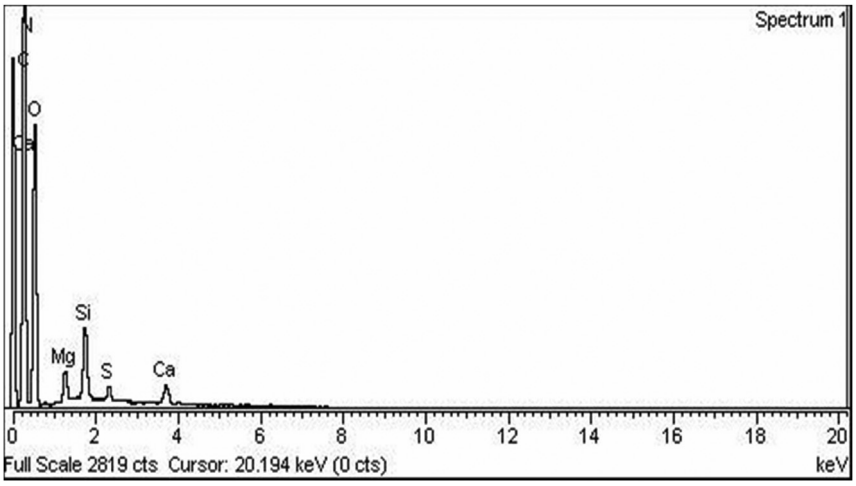

Figure 6 – EDX profile of formulation F9. EDX = energy dispersive X-ray.

Table 7 – Solubility study data of piroxicam-β-cyclodextrin in different solvents.

Solvent system	Solubility (mg/mL)	Solvent system	Solubility (mg/mL)
Water	6.61	Methanol/water (50:50)	4.18
Ethanol	2.83	Phosphate buffer of pH 7.4	23.90
Methanol	2.56	Phosphate buffer of pH 7.2	11.0
Acetone	1.40	Phosphate buffer of pH 7.0	9.0
Diethyl ether	0.80	Phosphate buffer of pH 6.8	3.50
Chloroform	0.90	Phosphate buffer of pH 1.2	1.50
Propylene glycol	3.96	Ethanol/phosphate buffer of pH 7.4 (50:50)	0.0099
Acetonitrile	4.0	Ethanol/phosphate buffer of pH 7.4 (40:60)	0.87
Ethyl acetate	3.0	Methanol/phosphate buffer of pH 7.4 (50:50)	0.0199
Dichloromethane	2.0	Diethyl ether/phosphate buffer of pH 7.4 (50:50)	0.50
Ethanol/water (50:50)	5.53	Acetone/phosphate buffer of pH 7.4 (50:50)	0.98

3.10. *Erosion studies*

The erosion study of nanocomposite films were performed in different buffer pH 1.2, 4.5 and 7.4, and results obtained are given in Table 9.

Table 9 shows that erosion studies of films were higher in pH 1.2 as compared to pH 4.5 and 7.4 regardless of the PEG grade used. It was observed that erosion studies were found maximum by decreasing the amount of chitosan. Formulation F10 showed the maximum weight loss (76.2 ± 0.56%) containing 75% PEG, whereas F1 showed the minimum weight loss (36.6 ± 0.85%) containing 0% PEG.

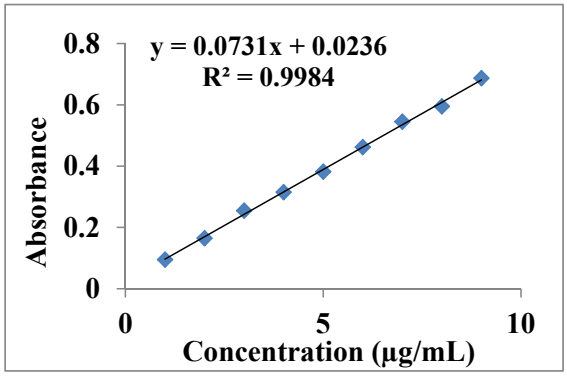

Figure 7 – Standard curve for piroxicam-β-cyclodextrin.

3.11. *Ex vivo permeation studies*

Ex vivo skin permeation studies of drug-loaded nanocomposite films containing different combinations of PEG and

Table 8 – Drug loading efficiency and drug content of piroxicam-β-cyclodextrin in the nanocomposite films.

Formulation codes	Contents in center (% ± SD)	Contents in proximity (% ± SD)
F1	93.72 ± 1.14	93.24 ± 1.96
F2	94.11 ± 0.06	94.39 ± 0.08
F3	95.27 ± 0.54	95.59 ± 0.49
F4	97.93 ± 0.65	97.26 ± 0.49
F7	93.72 ± 1.14	93.24 ± 1.96
F8	94.79 ± 0.76	94.84 ± 0.83
F9	97.41 ± 0.98	97.22 ± 0.72
F10	99.31 ± 0.44	99.66 ± 0.74
F13	93.78 ± 0.34	93.49 ± 0.52
F14	94.80 ± 1.98	94.39 ± 2.34
F15	95.09 ± 1.07	95.63 ± 2.01
F16	96.07 ± 2.19	96.46 ± 1.34
F17	93.72 ± 1.14	93.24 ± 1.96
F18	95.13 ± 0.22	95.54 ± 0.44
F19	96.47 ± 0.54	96.53 ± 0.66
F20	98.55 ± 0.44	98.82 ± 0.73

SD = standard deviation.

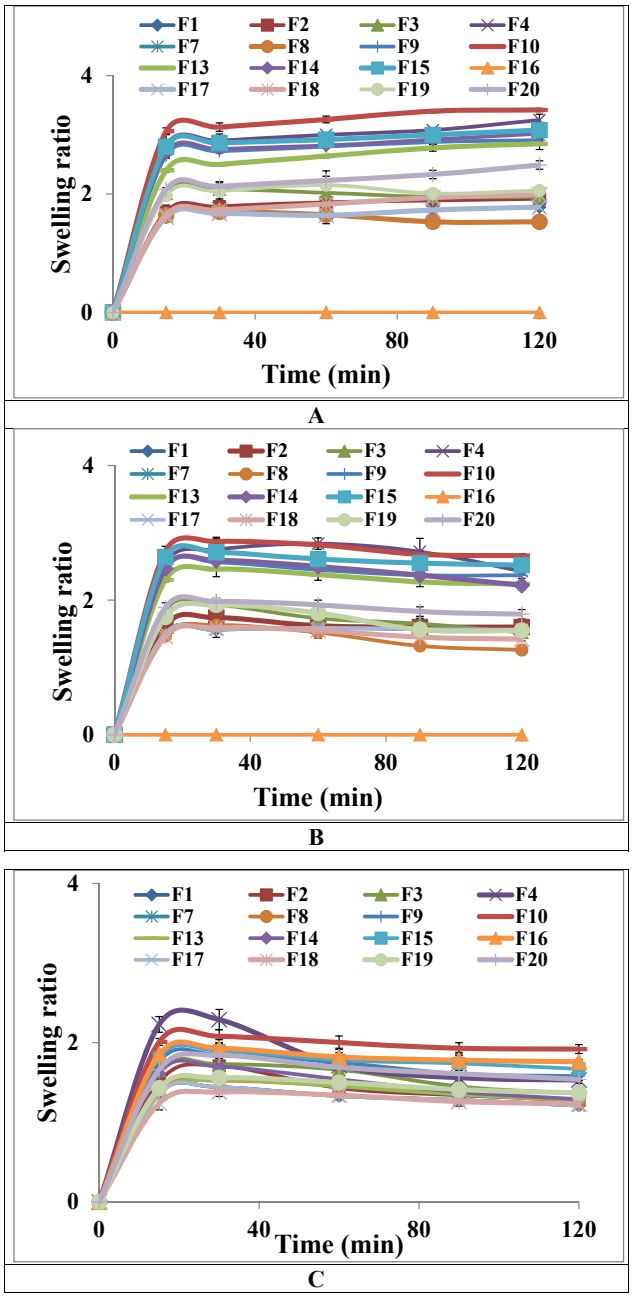

Figure 8 – Swelling ratio of chitosan–polyethylene glycol nanocomposite films. (A) HCl buffer, pH 1.2. (B) Acetate buffer, pH 4.5. (C) Phosphate buffer, pH 7.4.

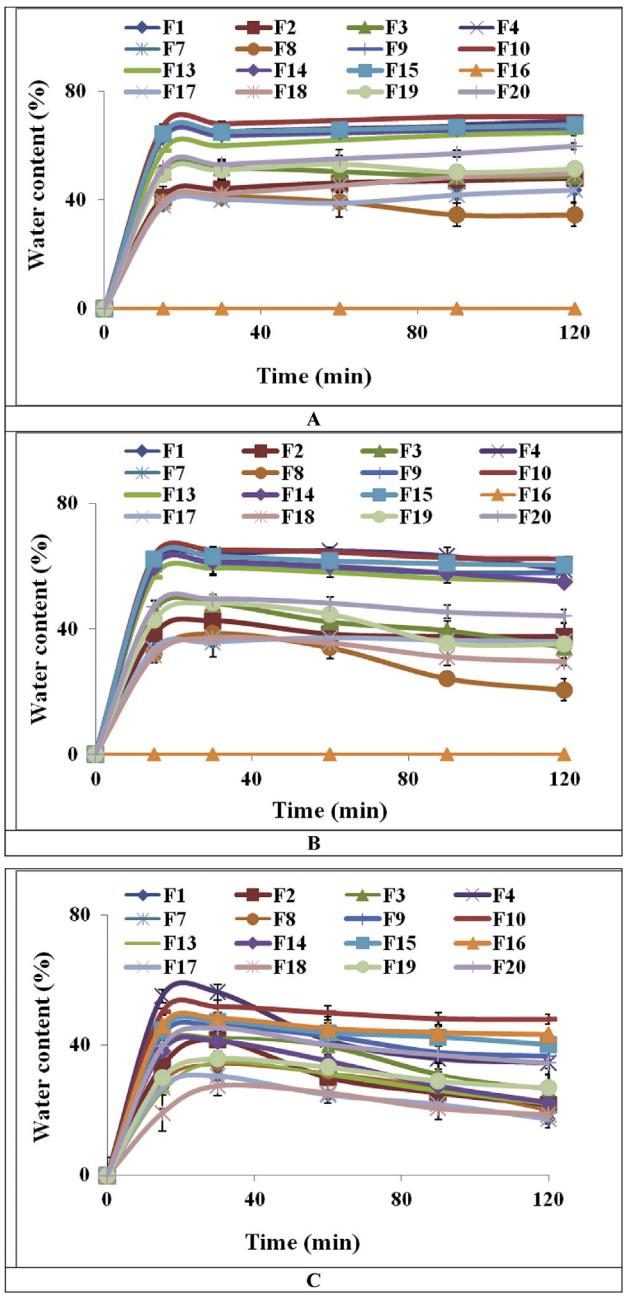

Figure 9 – Percentage water content of chitosan–polyethylene glycol nanocomposite films. (A) HCl buffer, pH 1.2. (B) Acetate buffer, pH 4.5. (C) Phosphate buffer, pH 7.4.

chitosan were performed by using Franz diffusion cells. Figure 10 shows the percentage of cumulative drug permeated from nanocomposite films.

It was observed that as we increased the concentration of chitosan, the drug permeation through rat skin was decreased. It is clear from Figure 10 that among all formulations, F10 (2405.15 ± 10.97 μg/cm^2) showed the highest cumulative drug permeation containing 75% PEG, whereas formulation F7 (1576.85 ± 11.81 μg/cm^2) showed lowest drug permeation containing 0% PEG. Because F10 had the highest flux (1.17 ± 0.004 μg/cm^2/min), permeability coefficient ($5.09 \times 10^{-4} \pm 1.70 \times 10^{-6}$ cm/min), and diffusion coefficient (0.44 ± 0.003 cm^2/min) as shown in Table 10, it was further evaluated by varying the glycerol concentration—i.e., 0%, 10%, 30%, and 70%—and it was observed that drug permeation through the skin was increased by decreasing the concentration of glycerol, but the maximum drug permeation was obtained from formulation F10 containing 50% glycerol.

Formulations F4, F10, and F20 containing 75% PEG and 25% chitosan were compared to evaluate the effect of the different molecular weights of PEG. The higher flux value was observed

Table 9 – Erosion studies of chitosan–polyethylene glycol nanocomposite films.

Formulation codes	Erosion (% ± SD)		
	pH 1.2	pH 4.5	pH 7.4
F1	36.60 ± 0.85	32.0 ± 0.28	29.90 ± 0.99
F2	53.0 ± 0.28	51.40 ± 0.85	47.50 ± 0.42
F3	57.10 ± 0.42	50.70 ± 0.42	45.20 ± 0.28
F4	65.10 ± 0.42	60.70 ± 0.71	57.50 ± 0.42
F7	36.60 ± 0.85	32.0 ± 0.28	29.90 ± 0.99
F8	56.70 ± 0.71	53.90 ± 1.55	48.10 ± 1.27
F9	59.70 ± 0.99	54.60 ± 1.13	50.30 ± 0.71
F10	76.20 ± 0.56	73.80 ± 0.85	69.90 ± 0.42
F13	59.20 ± 0.56	56.70 ± 0.71	55.20 ± 0.85
F14	68.80 ± 0.85	60.90 ± 0.99	58.90 ± 0.42
F15	68.90 ± 0.85	64.40 ± 0.56	59.70 ± 0.71
F16	0.0 ± 0.0	0.0 ± 0.00	63.20 ± 0.56
F17	36.60 ± 0.85	32.0 ± 0.28	29.90 ± 0.99
F18	49.10 ± 1.84	48.10 ± 1.83	43.40 ± 0.28
F19	60.70 ± 0.71	58.80 ± 0.85	54.50 ± 0.42
F20	69.30 ± 0.71	63.80 ± 0.56	59.20 ± 0.85

SD = standard deviation.

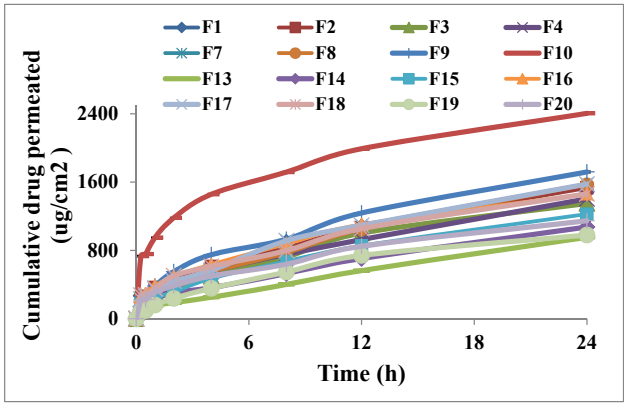

Figure 10 – Percentage cumulative drug permeated profile of piroxicam-β-cyclodextrin from nanocomposite films.

in PEG 2000, then in PEG 750, and finally in PEG 5000. The formulations containing PEG 2000 showed the maximum drug permeation through the skin as compared to PEG 750 and PEG 5000.

3.12. *Dissolution studies*

The release studies were performed to estimate the reproducibility of rate and duration of the drug release profile. The release of piroxicam-β-cyclodextrin from nanocomposite films was calculated as cumulative percent drug release. After 12 hours of dissolution, the cumulative percent drug release from nanocomposite films was greater than 35%. The cumulative drug release profiles for all formulations are shown in Figure 11.

As noted, when the amount of chitosan was decreased, maximum drug release was observed. Formulation F10, which contained 75% PEG, showed the maximum cumulative percent drug release (35.51 ± 0.26117%), whereas formulation F7, which contained 0% PEG, showed the minimum cumulative percent drug release (29.88 ± 0.29987%). Thus, F10 was further evaluated by varying the glycerol concentration (0%, 10%, 30%, and 70%), and it was found that percentage drug release had been increased by decreasing the concentration of glycerol, but maximum drug release was obtained from F10 containing 50% glycerol.

In vitro drug release kinetic models were applied to the noncomposite films of piroxicam-β-cyclodextrin using PEG 750, PEG 2000, and PEG 5000. All the selected kinetic models—i.e., zero-order, first-order, Higuchi model, and Korsmeyer–Peppas model—were applied properly to the data obtained from prepared nanocomposite films. The K and R^2 values obtained from zero-order, first-order, Higuchi model, and Korsmeyer–Peppas model are given in Table 11. It is clear from Table 11 that all formulations followed zero order as evident from the highest value of R^2, wherein R^2 values were in the range of 0.950–0.997 except in formulations F13, F14, and F20, which followed first order containing an R^2 value of 0.968–0.988. However, the R^2 values of zero order were nonsignificantly different from those of the first order ($R^2 = 0.933–0.988$). The drug release was also confirmed from the value of n obtained from the Korsmeyer–Peppas model. The value of n in the Korsmeyer–Peppas equation was found to be greater than 0.89 for all prepared formulations, which indicates that all formulations except F13, F14, and F20 were exhibiting super case II drug diffusion as shown in Table 11. The greater drug release was observed in HCl buffer pH 1.2 as compared to phosphate buffer having pH 6.8 and 7.4.

The formulations F4, F10, and F20 containing 75% PEG and 25% chitosan were compared to evaluate the effect of the different molecular weights of PEG. The higher K_0 value was observed in PEG 2000, then in PEG 750, and finally in PEG 5000. The formulations containing PEG 2000 released the drug faster compared to PEG 750 and PEG 5000.

The similarity factor (f_2) test was applied to compare formulations of the same composition with different viscosity grades of PEG, and results obtained are shown in Table 12. Formulation F2 containing 75% chitosan and 25% PEG 750 was compared with F8 containing 75% chitosan and 25% PEG 2000 and F18 containing 75% chitosan and 25% PEG 5000. It was found that all formulations were similar with each other, with f_2 value of 69.80–74.19, but the highest similarity factor (74.19) was found in F2 and F8. Formulation F3 containing 50% chitosan and 50% PEG 750 was compared with F9 containing 50% chitosan and 50% PEG 2000 and F19 containing 50% chitosan and 50% PEG 5000. It was observed that all formulations were similar with each other, with f_2 value of 71.60–70.83, but the highest similarity factor (71.60) was found in F3 and F9. Formulation F4 containing 25% chitosan and 75% PEG 750 was compared with F10 containing 25% chitosan and 75% PEG 2000 and F20 containing 25% chitosan and 75% PEG 5000. It was observed that all formulations are similar with each other, with f_2 value of 57.34–71.85, but the highest similarity factor (71.85) was found in F4 and F20. Formulation F8 containing 75% chitosan and 25% PEG 2000 was compared with formulation F18 containing 75% chitosan and 25% PEG 5000, formulation F9 containing 50% chitosan and 50% PEG 2000 was compared with formulation F19 containing 50% chitosan and 50% PEG 5000, and formulation F10 containing 25% chitosan and 75%

Table 10 – Calculated permeability parameters of nanocomposite films through rat skin.

Formulation codes	Flux ($\mu g/cm^2/min \pm SD$)	D ($cm^2/min \pm SD$)	K_p ($cm/min \pm SD$)
F1	0.95 ± 0.006	0.27 ± 0.001	$4.1 \times 10^{-4} \pm 2.9 \times 10^{-6}$
F2	0.90 ± 0.005	0.30 ± 0.001	$3.9 \times 10^{-4} \pm 2.29 \times 10^{-6}$
F3	0.85 ± 0.003	0.24 ± 0.0007	$3.6 \times 10^{-4} \pm 1.7 \times 10^{-6}$
F4	0.83 ± 0.004	0.22 ± 0.002	$3.7 \times 10^{-4} \pm 1.4 \times 10^{-6}$
F7	0.95 ± 0.006	0.27 ± 0.001	$4.1 \times 10^{-4} \pm 2.9 \times 10^{-6}$
F8	0.97 ± 0.005	0.23 ± 0.002	$4.24 \times 10^{-4} \pm 2.0 \times 10^{-6}$
F9	1.07 ± 0.006	0.27 ± 0.0004	$4.66 \times 10^{-4} \pm 2.6 \times 10^{-6}$
F10	1.17 ± 0.004	0.44 ± 0.003	$5.09 \times 10^{-4} \pm 1.7 \times 10^{-6}$
F13	0.61 ± 0.004	0.14 ± 0.0008	$2.65 \times 10^{-4} \pm 1.9 \times 10^{-6}$
F14	0.64 ± 0.006	0.24 ± 0.002	$2.79 \times 10^{-4} \pm 2.6 \times 10^{-6}$
F15	0.75 ± 0.005	0.24 ± 0.002	$3.27 \times 10^{-4} \pm 2.0 \times 10^{-6}$
F16	0.85 ± 0.004	0.35 ± 0.0009	$3.68 \times 10^{-4} \pm 1.8 \times 10^{-6}$
F17	0.95 ± 0.006	0.27 ± 0.001	$4.1 \times 10^{-4} \pm 2.9 \times 10^{-6}$
F18	0.83 ± 0.005	0.34 ± 0.001	$3.63 \times 10^{-4} \pm 2.2 \times 10^{-6}$
F19	0.65 ± 0.002	0.35 ± 0.004	$2.81 \times 10^{-4} \pm 1.8 \times 10^{-6}$
F20	0.65 ± 0.004	0.19 ± 0.004	$2.84 \times 10^{-4} \pm 1.1 \times 10^{-6}$

SD = standard deviation.

PEG 2000 was compared with formulation F20 containing 25% chitosan and 75% PEG 5000. It was observed that all formulations were similar with each other, with f_2 value of 59.86–60.91, but the highest similarity factor (60.91) was found in F9 and F19. When formulation F2 containing 75% chitosan and 25% PEG 750 was compared with formulation F3 containing 50% chitosan and 25% PEG 750 and F4 containing 25% chitosan and 75% PEG 750, it was observed that all formulations were similar with each other, with f_2 value of 88.34–90.20, but the highest similarity factor (90.20) was found in F2 and F3. Formulation F8 containing 75% chitosan and 25% PEG 2000 was compared with formulation F9 containing 50% chitosan and 25% PEG 2000 and F10 containing 25% chitosan and 75% PEG 2000. It was observed that all formulations were similar with each other having f_2 value 74.64–87.89 but the highest similarity factor (87.89) was found in F8 and F9. When formulation F1 containing 75% chitosan and 25% PEG 5000 was compared with formulation F19 containing 50% chitosan and 25% PEG 5000 and F20 containing 25% chitosan and 75% PEG 750, it was observed that all formulations were similar with each other, with f_2 value of 85.05–93.69, but the highest similarity factor (93.69) was found in F2 and F3.

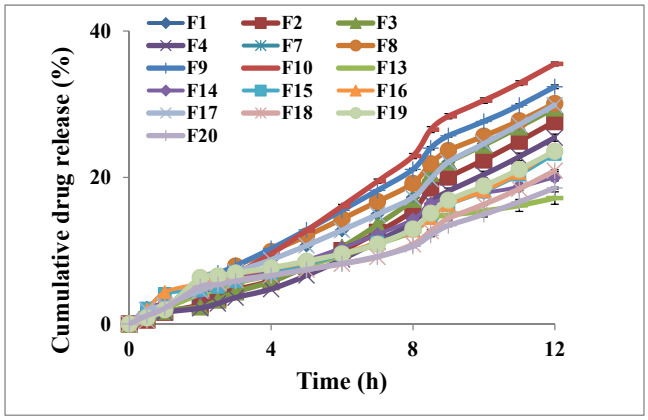

Figure 11 – Comparative *in vitro* release of piroxicam-β-cyclodextrin from nanocomposite films.

3.13. *Anti-inflammatory activity*

The anti-inflammatory activity of control, F4, F10, and F20 formulations were evaluated using carrageenan-induced hind paw edema method using rats as model. The results obtained after performing the anti-inflammatory activity are shown in Figure 12.

NSAIDs administered topically penetrate the skin slowly and enter the systemic circulation in small amounts. Figure 12 demonstrates that formulation F10 showed a significantly higher ($p < 0.0001$) anti-inflammatory effect as compared with the control, F4, and F20. High permeability indicates a greater amount of piroxicam-β-cyclodextrin available to generate an anti-inflammatory effect at the area of application of film.

4. Discussion

4.1. *Chemical interaction*

From the FTIR spectra of chitosan–PEG nanocomposite films in Table 3, it is observed that the stretching vibration of the N–H group bound to the O–H group moves to a lower wave number and becomes wider, indicating an increase in hydrogen bonding, which shows strong intermolecular interaction and good molecular compatibility between PEG and chitosan. In drug-loaded nanocomposite films, no new characteristic absorption bands are observed that shows no chemical reaction between drug and chitosan–PEG nanocomposites films. It is observed that piroxicam-β-cyclodextrin does not lose its activity in drug-loaded chitosan–PEG nanocomposite films [28].

From the TGA thermograms of chitosan–PEG nanocomposite films in Table 4, it is observed that chitosan–PEG 2000 has the maximum thermal stability as compared to chitosan–PEG 750 and PEG 5000, which is according to the

Table 11 – Dissolution kinetic model results for *in vitro* drug release profile of piroxicam-β-cyclodextrin from nanocomposite films.

Formulation codes	Zero order		First order		Higuchi model		Korsmeyer –Peppas		Results
	K_0	R^2	K_1	R^2	K_H	R^2	K_{KP}	n	Mechanism of release
F1	2.37	0.989	0.02	0.977	6.58	0.822	1.80	1.126	Super Case II Transport
F2	2.27	0.952	0.02	0.932	6.17	0.732	0.88	1.428	Super Case II Transport
F3	2.10	0.962	0.02	0.944	5.740	0.747	0.89	1.389	Super Case II Transport
F4	1.90	0.950	0.02	0.933	5.16	0.727	0.68	1.469	Super Case II Transport
F7	2.37	0.989	0.02	0.977	6.58	0.822	1.80	1.126	Super Case II Transport
F8	2.51	0.997	0.02	0.991	6.99	0.849	2.33	1.034	Super Case II Transport
F9	2.72	0.996	0.03	0.989	7.56	0.848	2.53	1.033	Super Case II Transport
F10	2.94	0.987	0.03	0.972	8.10	0.806	2.07	1.159	Super Case II Transport
F13	1.56	0.982	0.02	0.988	4.39	0.904	2.15	0.851	Anomalous
F14	1.78	0.984	0.02	0.988	5.01	0.891	2.27	0.888	Anomalous
F15	1.80	0.975	0.02	0.967	5.01	0.838	1.65	1.038	Super Case II Transport
F16	1.82	0.959	0.02	0.954	5.11	0.847	1.95	0.968	Super Case II Transport
F17	2.37	0.989	0.02	0.977	6.58	0.822	1.80	1.126	Super Case II Transport
F18	1.85	0.965	0.02	0.960	5.18	0.844	1.90	0.988	Super Case II Transport
F19	1.60	0.958	0.02	0.952	4.47	0.831	1.54	1.016	Super Case II Transport
F20	1.49	0.967	0.02	0.968	4.17	0.876	1.87	0.896	Case II Transport

Table 12 – Similarity values (f_2) obtained from dissolution profile of piroxicam-β-cyclodextrin from nanocomposite films.

Formulation comparison	f_2 value	Formulation comparison	f_2 value	Formulation comparison	f_2 value
F2 vs. F8	74.19	F3 vs. F9	71.60	F4 vs. F10	57.34
F2 vs. F18	69.80	F3 vs. F19	70.83	F4 vs. F20	71.85
F8 vs. F18	59.86	F9 vs. F19	60.91	F10 vs. F20	50.02
F2 vs. F3	90.20	F8 vs. F9	87.89	F18 vs. F19	85.05
F2 vs. F4	88.34	F8 vs. F10	74.64	F18 vs. F20	93.69

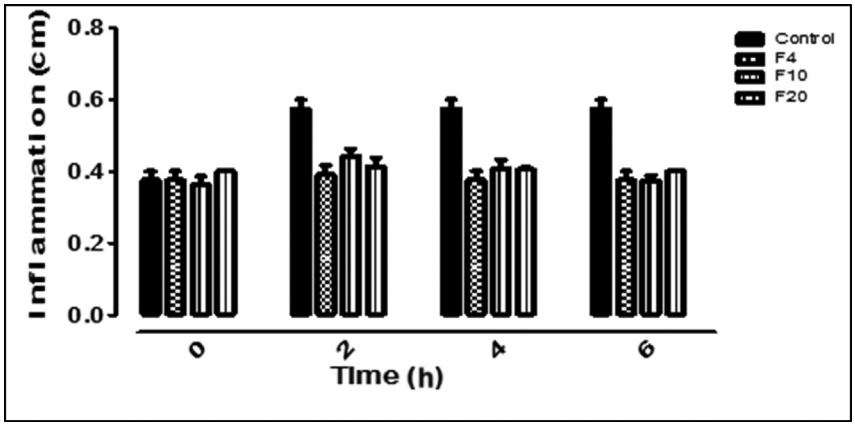

Figure 12 – Topical administration effect of different formulations of piroxicam-β-cyclodextrin on rat right hind paw after administration of carrageenan injection.

literature [29]. Previous studies have shown that both PEG and chitosan are crystalline [28]. Piroxicam itself is also crystalline in nature, but it loses its crystallinity when it complexes with β-cyclodextrin [30]. Figure 3 shows that with the addition of drug, chitosan–PEG nanocomposites lose their crystallinity.

4.2. *Preliminary solubility studies of piroxicam-β-cyclodextrin*

β-Cyclodextrin are chemically stable, water-soluble compounds that form complexes with water-insoluble (lipophilic) molecules [30]. They have been recognized as the most important group of pharmaceutical excipients enhancing/improving the drug solubility and bioavailability of poorly water soluble drugs. Piroxicam itself is a weakly acidic drug, less water soluble, and poorly absorbed from the gastrointestinal tract [14]. In the case of piroxicam-β-cyclodextrin complex, piroxicam loses its crystal structure and becomes a more hydrophilic and rapidly wettable compound that dissolves rapidly in water [30]. The drug is found to be most soluble in phosphate buffer of pH 7.4, as the acidic nature of piroxicam-β-cyclodextrin allows its solubility to enhance with

the increase in pH [31]. The drug is found to be highly soluble in phosphate buffer of pH 7.4 (23.90 mg) than in pH 7.2 (11.0 mg), pH 7 (9.0 mg), pH 6.8 (3.5.0 mg), and HCl buffer pH 1.2 (1.5 mg), as shown in Table 7. Thus, this solvent system is recommended to be selected for further studies.

4.3. *Swelling studies and water content*

The swelling behavior depends on the nature of the polymer and its solvent compatibility [7]. The results predicts that pH 1.2 allows the highest swelling rate in comparison to pH 4.5 and 7.4, owing to the inherent hydrophobic nature of chitosan that prevents rapid swelling in alkaline and neutral pH because chitosan is not soluble in neutral or basic pH range and dissolves in specific organic and inorganic solvents. The maximum swelling ratio is found in formulations containing PEG 2000 as compared to PEG 750 and PEG 5000 because permeability of water depends on pore size and porosity, resulting in maximum permeability of water [32]. The formulations containing high PEG concentration shows rapid swelling of nanocomposites because of high diffusivity of PEG in water [33] as PEG is amphiphilic and dissolves both in aqueous and organic solvents [34].

Formulation F16 is decomposed during swelling studies in HCl buffer pH 1.2 and acetate buffer pH 4.5 owing to the absence of glycerol, as the presence of glycerol provides higher dimensional stability to the formulation because of the formation of the crosslink network generated by hydrogen bonding between glycerol and chitosan [35].

4.4. *Ex vivo permeation studies*

pH plays vital role in the activity of topical preparations of NSAIDs. If pH has been gradually increased, different NSAIDs will show about 10-fold increase in their flux. The ion pairing effect plays a significant role in the absorption of NSAIDs because these drugs make an ionic bond with external skin components such as fatty acids, as a result of which the ion pair complex would be more lipophilic. Piroxicam also forms an ion pair complex with buffer components (sodium hydroxide and potassium dihydrogen phosphate), resulting in increased lipophilicity and good penetration. In comparison with passive diffusion, the flux of piroxicam can also be increased when combined with β-cyclodextrin [14]. F10 shows the maximum drug permeation through rat skin (2405.15 ± 10.97 μg/cm^2) because it contains 75% PEG (PEG acts as a soluble macromolecule, so it dissolves and forms pores, which increases drug penetration through the skin) [28]. The formulations containing PEG 2000 shows the maximum permeation of drug as the permeability of porous material is estimated by its porosity and pore size. The high permeability of PEG 2000 may be attributable to its highest porosity [32].

4.5. *Dissolution studies*

The amount of drug release is found maximum in acidic solution than in basic solution because the drug release rate depends on the swelling of nanocomposite films. The greater drug release is observed in buffer of pH 1.2 as compared to phosphate buffer of pH 6.8 and 7.4 because of the electrostatic interaction between anions and chitosan, which is considerably affected by the pH level of the medium that ultimately results in the rapid release of drug at low pH. The salt bonds and ionic crosslinking become weaker at lower pH medium and thus facilitate the swelling of film and increases drug release. Formulation F10 shows the maximum percentage drug release (35.51%) because it contains 75% PEG [28].

5. Conclusion

Film composition had a particular impact on drug release properties. It is possible to alter the swelling of films, drug release, and permeation rate by changing the composition of chitosan–PEG in nanocomposite films. The different molecular weights of PEG have a strong influence on swelling, drug release, and permeation rate. PEG 2000 showed the highest value of swelling, flux, and K_0 value as compared to PEG 750 and PEG 5000. The drug holding capacity of PEG 2000 was found to be the lower than that of PEG 750 and PEG 5000.

Conflicts of interest

There is no conflict of interest over the contents of this article.

REFERENCES

[1] Alai MS, Lin WJ, Pingale SS. Application of polymeric nanoparticles and micelles in insulin oral delivery. J Food Drug Anal 2015;23:351–8.
[2] Shah SU, Shah KU, Rehman A, Khan GM. Investigating the in vitro drug release kinetics from controlled release diclofenac potassium–ethocel matrix tablets and the influence of co-excipients on drug release patterns. Pak J Pharm Sci 2011;24:183–92.
[3] Zheng Y, Monty J, Linhardt RJ. Polysaccharide-based nanocomposites and their applications. Carbohydr Res 2015;405:23–32.
[4] Camargo PHC, Satyanarayana KG, Wypych F. Nanocomposites: synthesis, structure, properties and new application opportunities. Mater Res 2009;12:1–39.
[5] Oliveira M, Machado A. Preparation of polymer-based nanocomposites by different routes. In: Nanocomposites: synthesis, characterization and applications. Portugal: NOVA Publishers; 2013. p. 1–22.
[6] Salehifar M, Beladi NM, Alizadeh R, Azizi MH. Effect of LDPE/MWCNT films on the shelf life of Iranian Lavash bread. Pelagia Res Libr 2013;3:183–8.
[7] Wu SH, Sun NN, Chau CF. Microspheres as carriers for lipase inhibitory substances to reduce dietary triglyceride absorption in mice. J Food Drug Anal 2016;24:129–35.
[8] Wang Q, Dong Z, Du Y, Kennedy JF. Controlled release of ciprofloxacin hydrochloride from chitosan/polyethylene glycol blend films. Carbohydr Polym 2007;69:336–43.
[9] Elgadir MA, Uddin MS, Ferdosh S, Adam A, Chowdhury AJK, Sarker MZI. Impact of chitosan composites and chitosan nanoparticle composites on various drug delivery systems: a review. J Food Drug Anal 2015;23:619–29.
[10] Xu Y, Ren X, Hanna MA. Chitosan/clay nanocomposite film preparation and characterization. J Appl Polym Sci 2006;99:1684–91.

[11] Feldman D. Polyblend Nanocomposites. J Macromol Sci 2015;52:648–58.
[12] Kotal M, Bhowmick AK. Polymer nanocomposites from modified clays: recent advances and challenges. Prog Polym Sci 2015;51:127–87.
[13] Ruiz-Hitky E, Darder M, Alcantara AC, Wicklein B, Aranda P. Recent advances on fibrous clay-based nanocomposites. Adv Polym Sci 2015;267:39–86.
[14] Shah SNH, Rabbani ME, Shahzad Y, Badshah A, Meidan VM, Murtaza G. Developing an efficacious diclofenac diethylamine transdermal formulation. J Food Drug Anal 2012;20:464–70.
[15] Reginster JY, Franchimont P. Piroxicam-beta-cyclodextrin in the treatment of acute pain of rheumatic disease. Eur J Rheumatol Inflamm 1992;12:38–46.
[16] Lee CR, Balfour JA. Piroxicam-β-cyclodextrin. Drugs 1994;48:907–29.
[17] Hussein AA, Mahmood HSh. Preparation and evaluation of cefixime nanocrystals. Iraqi J Pharm Sci 2014;23:1–12.
[18] Mohanty DP, Biswal S, Nayak L. Preparation of starch–chitosan nanocomposites for control drug release of curcumin. Int J Curr Eng Technol 2015;5. 336–31.
[19] Liu H, Adhikari R, Guo Q, Adhikari B. Preparation and characterization of glycerol plasticized (high-amylose) starch–chitosan films. J Food Eng 2013;116:588–97.
[20] Khunt DM, Mishra AD, Shah DR. Formulation design & development of piroxicam emulgel. Int J PharmTech Res 2012;4:1332–44.
[21] Dol H, Gandhi S, Pardhi D, Vyawahare N. Formulation and evaluation of in situ ophthalmic gel of moxifloxacin hydrochloride. Pharma Innovation 2014;3:60–6.
[22] Cao Z, Yang Q, Fan C, Liu L, Liao L. Biocompatible, ionic-strength-sensitive, double-network hydrogel based on chitosan and an oligo(trimethylene carbonate)–poly(ethylene glycol)–oligo(trimethylene carbonate) triblock copolymer. J Appl Polym Sci 2015;132:42459–66.
[23] Lamoudi L, Chaumeil JC, Daoud K. Swelling, erosion and drug release characteristics of sodium diclofenac from heterogeneous matrix tablets. J Drug Deliv Sci Technol 2016;31:93–100.
[24] Csóka I, Csányi E, Zapantis G, Nagy E, Fehér-Kiss A, Horváth G, Blazsó G, Erős I. In vitro and in vivo percutaneous absorption of topical dosage forms: case studies. Int J Pharm 2005;291:11–9.
[25] Chaudhary H, Rohilla A, Rathee P, Kumar V. Optimization and formulation design of carbopol loaded Piroxicam gel using novel penetration enhancers. Int J Biol Macromol 2013;55:246–53.
[26] Gaur PK, Mishra S, Bajpai M. Formulation and evaluation of controlled-release of telmisartan microspheres: in vitro/in vivo study. J Food Drug Anal 2014;22:542–8.
[27] Monton C, Charoenchai L, Suksaeree J, Sueree L. Quantitation of curcuminoid contents, dissolution profile, and volatile oil content of turmeric capsules produced at some secondary government hospitals. J Food Drug Anal 2016;24:493–9.
[28] Wang Q, Zhang N, Hu X, Yang J, Du Y. Chitosan/polyethylene glycol blend fibers and their properties for drug controlled release. J Biomed Mater Res A 2008;85:881–7.
[29] Gupta B, Saxena S, Arora A, Sarwar Alam M. Chitosan–polyethylene glycol coated cotton membranes for wound dressings. Indian J Fibre Text 2011;36:272–80.
[30] Scarpignato C. Piroxicam-β-cyclodextrin: a GI safer piroxicam. Curr Med Chem 2013;20:2415–37.
[31] Bettini R, Santi P, Catellani P, Massimo G, Bellotti A, Barthélémy C, Guyot-Hermann AM, Trublin F, Colombo P. Permeation of piroxicam and piroxicam-β-cyclodextrin through artificial membranes. Eur J Pharm Biopharm 1992;38:203–8.
[32] Zeng M, Fang Z, Xu C. Novel method of preparing microporous membrane by selective dissolution of chitosan/polyethylene glycol blend membrane. J Appl Polym Sci 2004;91:2840–7.
[33] Gupta K, Kumar MNR. pH dependent hydrolysis and drug release behavior of chitosan/poly(ethylene glycol) polymer network microspheres. J Mater Sci Mater Med 2001;12:753–9.
[34] Chan P, Kurisawa M, Chung JE, Yang YY. Synthesis and characterization of chitosan-g-poly(ethylene glycol)–folate as a non-viral carrier for tumor-targeted gene delivery. Biomaterials 2007;28:540–9.
[35] Lavorgna M, Piscitelli F, Mangiacapra P, Buonocore GG. Study of the combined effect of both clay and glycerol plasticizer on the properties of chitosan films. Carbohydr Polym 2010;82:291–8.